

**VOLCANIC ORIGIN OF FLAT FLOORED, BEDROCK CONTAINING CRATERS ON MARS.** C. S. Edwards<sup>1</sup>, A. D. Rogers<sup>2</sup>, J. L. Bandfield<sup>3</sup>, P. R. Christensen<sup>1</sup>, <sup>1</sup>Mars Space Flight Facility, Arizona State University, PO BOX 876305, Tempe, AZ, 85287-6305, [christopher.edwards@asu.edu](mailto:christopher.edwards@asu.edu), <sup>2</sup>Department of Geosciences, Stony Brook University, Stony Brook, NY, <sup>3</sup>Department of Earth and Space Sciences, University of Washington, Seattle, WA.

**Introduction:** High thermal inertia or bedrock instances have been identified and classified by *Edwards et al.* [1]. An exhaustive search of Thermal Emission Imaging System (THEMIS) [2] nighttime temperature data converted to thermal inertia using the KRC thermal model [3] has been conducted. In this study, high thermal inertia surfaces or interpreted bedrock are defined as a single pixel in a THEMIS image with a thermal inertia  $> 1200 \text{ J K}^{-1} \text{ m}^{-2} \text{ s}^{-1/2}$ , which may refer to either *in situ* bedrock exposures or other rock dominated surfaces. Either way, these surfaces represent what are likely the least weathered, both physically and chemically, materials on Mars [1]. Three distinct surface types have been identified including valley and crater walls, crater floors, and intercrater plains surfaces. The focus of this study is to better constrain the compositional variability of bedrock containing crater floors on Mars as compared to the surrounding regolith material.

*Rogers et al.* [4] have characterized a representative section of the martian southern highlands in Mare Serpentis. In this case, the region was limited geographically to an area where many surfaces of elevated thermal inertia (e.g.  $>600 \text{ J K}^{-1} \text{ m}^{-2} \text{ s}^{-1/2}$ ) were observed [4]. *Rogers et al.* [4] have determined in Mare Serpentis, that relatively high thermal inertia surfaces are commonly more mafic (e.g. more olivine and pyroxene rich) than the surrounding plains material. They propose two possibilities for the formation of these surfaces: 1) they are lithologically distinct and are fundamentally derived from different source materials, or 2) they are the products of weathering, where all the material began with a similar composition and older materials are altered to the compositions [5] observed by Thermal Emission Spectrometer (TES) data [6].

We have elected to take a different approach than *Rogers et al.* [4], where we have not constrained the area of interest by geographic location but rather by thermal inertia value, examining only those instances identified as bedrock, and further limiting the study to bedrock containing craters. These craters are on average  $\sim 52 \text{ km}$  in diameter, but range in size from  $18.5 \text{ km}$  to  $179 \text{ km}$ . They commonly lack a central peak, have shallow sloped walls, and no easily visible ejecta. These observations indicate the relatively old ages of these impacts as compared to many of the less modified craters commonly observed on Mars. Figure 1 illustrates a typical floor morphology for bedrock containing craters. Little to no aeolian material is typi-



**Figure 1.** HiRISE image (PSP\_00412\_0550) displaying the common morphology associated with bedrock containing craters.

cally observed, and these surfaces are commonly highly fractured.

**Data Analysis:** In order to assess the compositional variation across bedrock containing craters, several instruments have been utilized including THEMIS, Compact Reconnaissance Imaging Spectrometer (CRISM) [7] and TES data. In addition to compositional variability, morphologic textures have been examined using High Resolution Imaging Science Experiment (HiRISE) data [8]. Here we have provided an example site centered near  $46^\circ \text{E}$ ,  $25^\circ \text{S}$ .

**THEMIS.** Olivine bearing materials are easily discriminated in THEMIS decorrelation stretch images (Figure 2) as olivine has a large absorption feature centered in THEMIS band 7. This compositional data allows for a rapid qualitative examination of the distribution and contexts of olivine enriched materials as related to bedrock crater floors. Commonly, the most olivine-enriched materials are observed in floors these craters.

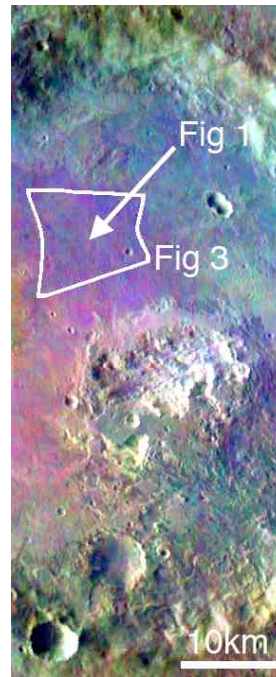


**Figure 2.** THEMIS decorrelation stretch (bands 8,7,5) image (I15052002) of an example high thermal inertia crater floor. In this band combination, purple indicates the presence of olivine-enriched materials.

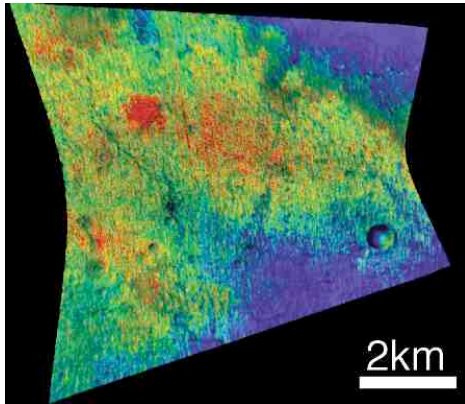


**Figure 3.** CRISM olivine index image (FRT000A102\_07). This image shows excellent correlation with THEMIS data, where both data are in agreement.

*CRISM.* Olivine enriched materials are commonly observed in CRISM data where THEMIS decorrelation stretch data identify olivine materials. Figure 3 illustrates the utility of higher resolution data, where it is observed that the highest olivine abundances (red tones) are associated with the roughest material. This is also often true of thermal inertia data, where the highest values are associated with the roughest terrain [1].

*TES.* Neither of the previous datasets can provide accurate quantitative mineralogical abundances for these sites. While TES data cannot provide the required morphologic information, they play a vital role in quantitatively characterizing the compositions of these surfaces. In Figure 4, Spectral un-mixing following *Ramsey and Christensen* [9] of the high thermal inertia material results in mineral abundances of ~38% plagioclase, ~13% orthopyroxene, ~20% clinopyroxene, and ~20% olivine, while the un-mixing of the surrounding plains material results in a much less mafic character with ~35% plagioclase, ~11% orthopyrox-

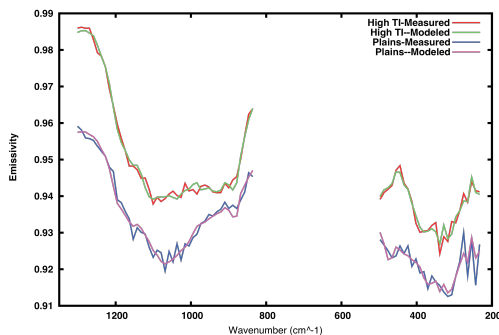


**Figure 4.** Averages of many TES spectra of this region and the respective model fits. Associated abundances are quoted in text.

ene, ~15% clinopyroxene, and ~7% olivine with the addition of ~20% high-Si phases. These differences are significant and common throughout the ~60 sites examined, though the modeled abundances and mineral suites vary from site to site.

**Discussion:** The composition of these craters in addition to morphologic evidence provide useful constraints to help understand the origin of bedrock containing craters. Here we propose that the formation of these craters is due to inflationary volcanism associated with the impact event. In this model, a sill or dike from a near by pre-existing magma chamber or a new magma body created by the unloading and partial melting of the underlying crust and mantle, intersects the fractured zone beneath the impact site. A new sill begins to form at the base of the highly fractured basement rock, which begins to inflate and lift the floor of the crater, fed by the tapped magma body [10]. If the fracturing of the basement rock is significant enough, then the magma can erupt onto the surface as lava flows and may entirely obscure the central peak of the crater. A similar hypothesis has been proposed for relatively large lunar craters [10, 11].

The compositional data in this study further support this hypothesis that is based largely on morphologic data, as most of the high thermal inertia material in these crater floors is significantly more mafic than the surrounding terrain. This may either indicate that the eruptive events that flooded the crater floors are compositionally distinct from the surrounding low inertia material or that this is the typical composition of martian lavas that erupted more recently in compared to the weathered regolith material.

Crater floors with elevated thermal inertia values (though lower than the defined bedrock value) are commonly observed throughout the cratered southern highlands, and may indicate a widespread process that has occurred in martian history.

#### References:

- [1] C. S. Edwards, J. L. Bandfield, R. L. Fergason, P. R. Christensen, (2009) *J. Geophys. Res.* **114**.
- [2] P. R. Christensen *et al.*, (2003) *Science* **300**, 2056.
- [3] H. H. Kieffer, (in prep).
- [4] A. D. Rogers, O. Aharonson, J. L. Bandfield, (2009) *Icarus* **200**, 446.
- [5] J. L. Bandfield, A. D. Rogers, (2008) *Geology* **36**, 579.
- [6] P. R. Christensen *et al.*, (2001) *J. Geophys. Res.* **106**, 23.
- [7] S. Murchie *et al.*, (2007) *J. Geophys. Res.* **112**.
- [8] A. S. McEwen *et al.*, (2007) *J. Geophys. Res.* **112**, E05S02.
- [9] M. S. Ramsey, P. R. Christensen, (1998) *J. Geophys. Res.* **103**, 577.
- [10] P. H. Schultz, (1976) *Earth, Moon, and Planets* **15**, 241.
- [11] P. H. Schultz, H. Glicken, (1979) *J. Geophys. Res.* **84**, 8033.